J. Plasma Fusion Res. SERIES, Vol. 3 (2000) 192–196

Structure of Edge Magnetic Field in Heliotron J

MIZUUCHI Tohru*, NAKASUGA Masahiko[1], SANO Fumimichi, NAKAMURA Yuji[1], KONDO Katsumi[1], OKADA Hiroyuki, NAGASAKI Kazunobu, BESSHOU Sakae[1], WAKATANI Masahiro[1] and OBIKI Tokuhiro

Institute of Advanced Energy, Kyoto University, Gokasho, Uji, 611-0011 Japan

[1]Graduate School of Energy Science, Kyoto University, Gokasho, Uji, 611-0011 Japan

(Received: 18 January 2000 / Accepted: 12 April 2000)

Abstract

Characteristics of edge magnetic field in a helical axis heliotron device, Heliotron J, are numerically investigated. Owing to the flexibility of field configuration control, helical or island divertor configurations can be realized in the same device. In the helical divertor configuration, the divertor footprints on the wall are localized in some discrete regions in a torus. Two different modes, m/n = 8/4 and 7/4, of island divertor configurations are appeared depending on the rotational transform near the outermost magnetic surface, $\iota/2\pi \sim 0.5$ and 0.57, respectively. In the latter configuration, the center of island is far from the confinement region. A part of the island crosses the wall and the footprints of field lines are localized on two regions per field period at low field side. In the m/n = 8/4 configuration, the center of island is close to the confinement region and the island does not cross the wall. In these divertor configurations, parallel and anti-parallel flows of SOL plasma reach at different areas on the wall (or divertor plates), respectively.

Keywords:

helical axis heliotron, Heliotron J, helical divertor, island divertor, edge field structure

1. Introduction

Divertor concept is essential for a high power and long pulse operation of fusion plasmas. In stellarator/heliotron devices, the structure of edge magnetic field is strongly affected by "natural islands" near the outermost magnetic surface (OMS). Based on a difference of the topology of edge field structure, two types of divertor configuration are proposed; helical and island divertors. In the former, the OMS is surrounded by "ergodic" filed lines, instead of a magnetic island chain in the latter. Although some experiments have investigated divertor plasma properties for each configuration in different devices, the experimental data is not enough to make detailed simulation models and to discuss advantages and disadvantages of each divertor scenario. More detailed experimental studies, especially comparative studies of the both types of divertor in the same device, are required to understand the characteristics of each divertor.

In Heliotron J, which is a helical axis heliotron device newly constructed at Institute of Advanced Energy of Kyoto University, it is possible to create several types of edge structure by changing current ratio of the coil system. This will give us a good opportunity for investigation of the edge structure effects on SOL and divertor plasmas. This paper discusses the characteristics of divertor configuration obtainable in Heliotron J.

2. The Heliotron J Device

Heliotron J is newly designed aiming to reduce the

Corresponding author's e-mail: mizuuchi@iae.kyoto-u.ac.jp

neoclassical transport and achieve higher <β> with small bootstrap current [1-3]. The main device parameters are R = 1.2 m, $<a_p> \approx$ 0.12–0.20 m, $B \leq$ 1.5 T and $\iota/2\pi \approx$ 0.4–0.8. The coil system of this device consists of an l = 1/m = 4 helical coil with pitch modulation of –0.4, two types of toroidal coils and three pairs of poloidal coils. Heliotron J is a low shear device and the edge field structure is very sensitive to the change of $\iota/2\pi$ resulting from variations of magnetic field components, which can be controlled in a wide range. Examples of the radial profile of $\iota/2\pi$ for some cases of the AV-coil current I_{AV} and the IV-coil current I_{IV} are shown in Fig.1. Three cases in the figure (A, B and C) are discussed in this paper. In Case A, $\iota/2\pi$ at the OMS is far from any low mode rational number. No clear island structure is observed in this case. In Cases B and C, $\iota/2\pi$ is close to n/m = 4/7 and 4/8, respectively and a clear island chain is observed outside the OMS. The details are described in the following section.

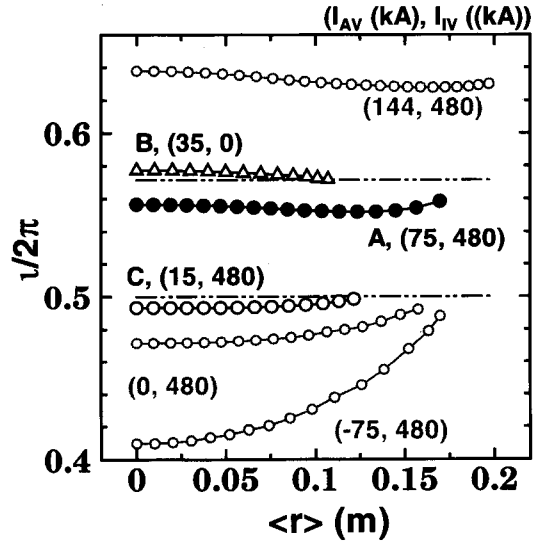

Fig. 1 Radial profile of $\iota/2\pi$ for some cases of I_{AV} and I_{IV}. Coil currents for other coils are I_H = 960 kA, I_V = –840 kA, I_{TA} = 500 kA, and I_{TB} = 200 kA.

3. Properties of the Edge Field Structure in Heliotron J

Figure 2 shows Poincaré plots of vacuum field lines on a poloidal cross-section for the three configurations shown in Fig. 1. For the edge region, the field lines on virtual magnetic surfaces outside the OMS are traced within a region of 0.7 m $\leq R \leq$ 1.7 m and –0.5 m $\leq Z \leq$ 0.5 m.

In Case A, the OMS is surrounded by "ergodic" field lines. This is similar to the case of conventional heliotron such as Heliotron E, which has a helical divertor configuration. From this point of view, we call this configuration a helical divertor configuration in this paper.

In Cases B and C, a clear island chain is observed outside the OMS. These configurations are candidates for an island divertor.

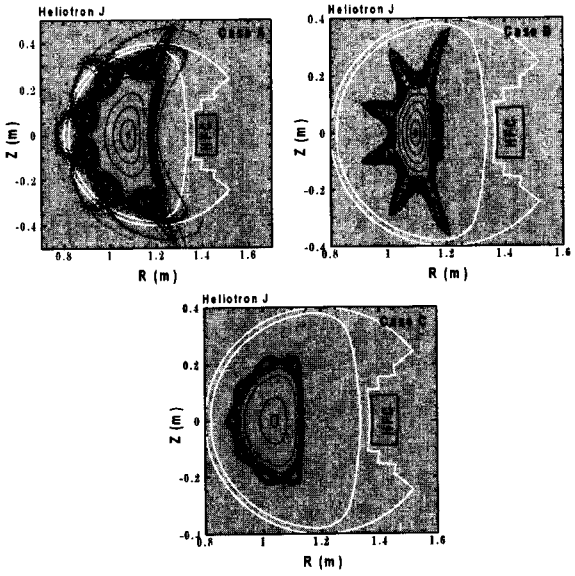

Fig. 2 Poincaré plots on a poloidal cross-section at a toroidal angle of φ = 45° for Case A, Case B and Case C shown in Fig. 1. White lines in each figure indicate the vacuum vessel.

3.1 Helical divertor configuration in Heliotron J

In order to discuss edge plasma behavior diffusing from the confinement region, it is enough to trace field lines from the core edge region to the wall surface of the vacuum vessel. Under this condition, the structure becomes simple since the field lines starting the core edge region cross the wall before the so-called "fold and stretch" effect becomes noticeable.

Figure 3(a) shows a Poincaré plot at φ = 67.5°, where the edge field lines cross the wall. In this figure, the results of tracing field lines starting from the virtual flux surface (5.0 mm outside the OMS) are plotted. As shown in this figure, only one "divertor leg" reaches to the wall at this toroidal position. The divertor footprints are plotted in Fig. 3(b). As in Fig. 3(b), the divertor footprints are localized not only in poloidal direction but also in toroidal direction. This stands in contrast to the

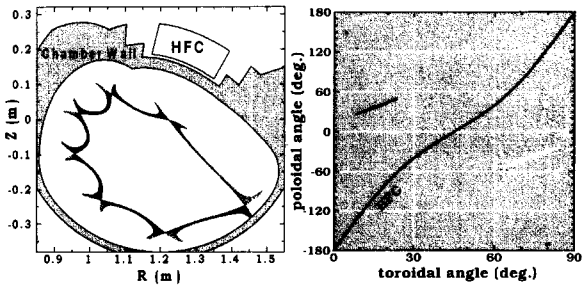

Fig. 3 (a) Poincaré plot of edge field lines within the vacuum chamber at φ = 67.5° for Case A. (b) Divertor footprint on the wall. (Note the toroidal angle of one period is 90°.)

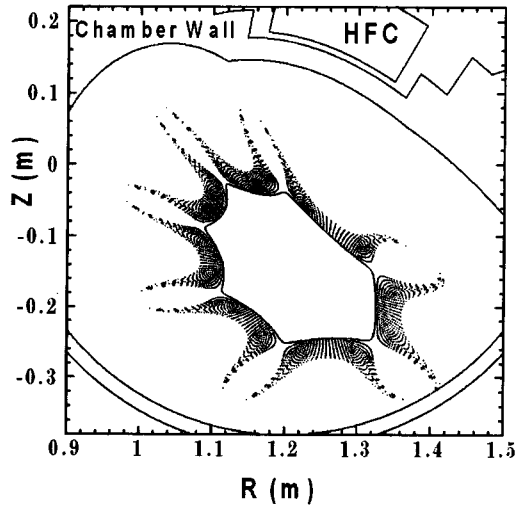

Fig. 4 Poincaré plot of edge field lines within the vacuum chamber at φ = 67.5° for Case B.

helical divertor in Heliotron E [4], where the divertor trace continuously runs along the torus helically. The different color in Fig. 3(b) denotes the difference in the direction of the field trace. It is expected that the diffused plasma from the core region go to the wall divided into parallel and anti-parallel flows to the field line. This is convenient to investigate divertor plasma physics such as plasma flow and/or SOL current and also to study divertor biasing effects, etc.

3.2 Island divertor configurations

As shown in Fig. 2, two different modes of island structure, Case B and Case C, are obtained for different values of the edge rotational transform.

In Case B, the center of the islands (O-point) is far from the confinement region. Although the basic mode of this island is m/n = 7/4, a detailed survey of the field topology shows that some other islands exist around the main island.

Taking into account the wall position, it is shown that the island magnetic fields cross the wall surface before they make a complete island (Fig. 4). The footprints of edge field lines are discrete in toroidal direction and the parallel and anti-parallel divertor plasma flows hit separate regions also in this case. The footprints are localized only at the low field side in this case. The footprints can be moved to the high field side by setting a target plate at the high field side. This makes it possible to examine effects of the mirror ratio near the target on the edge particle/heat transports.

As compared with Case A, this configuration has a long connection length (The connection length of the divertor field lines in Case B is one-order longer than Case A.) and it has long divertor legs, which is corresponding to a high X-point (or long X-point distance) divertor in tokamaks.

In the Case C configuration, the O-point of the island is close to the confinement region and there are closed surfaces outside the island chain (not shown in Fig. 2). However the wall scrapes these surfaces. The island itself does not cross the wall. By setting target plates at the island position, this configuration can be used as an island divertor such as the divertor proposed in W7-X. Although the island size is not so large and the mode of the island (n/m = 4/8) is rather high compared to LID in LHD (n/m = 1/1), an LID-type divertor might be possible to design.

4. Diffusion Effects

As the first step to evaluate effects of particle diffusion across the field line traveling from the OMS to the wall, a random walk process is included in the field trace calculation instead of a particle motion analysis. Examples of such calculations for three cases A and B are shown in Fig. 5, where the calculation is performed for ~ 200 field lines started on the OMS. The parameters of the random walk process are adjusted to correspond to the effective perpendicular diffusion coefficient of D $\approx$ 1 m^2/s. White dots for Cases A and B shows the results of tracing without "diffusion" for field lines starting from a virtual surface of 5.0 mm outside the OMS.

In Case A, as expected from its short connection length, the diffusion effect on the width of the divertor legs is not important. In Case B, due to the long connection length, the diffusion expands the width of

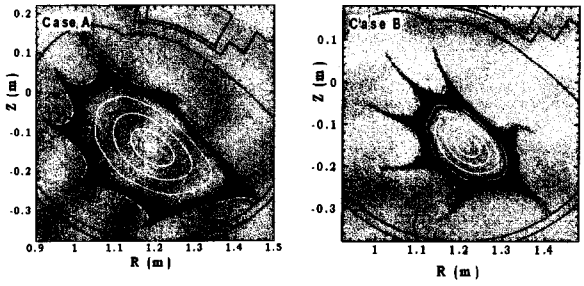

Fig. 5 Poincaré plots of edge field lines with a random walk process for Cases A and B.

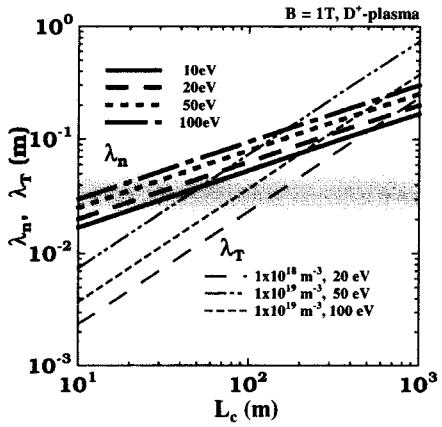

Fig. 6 Characteristic thickness of density λ_n and temperature λ_T in SOL vs. the connection length of the edge field line.

divertor plasma in the poloidal direction.

In Case C, since the O-point is close to the core region, target plates must be set near the OMS. In this case, the comparison of the SOL plasma thickness λ and the island size δ is important. Good points of island divertor configuration is valid when $\delta > \lambda$. Figure 5 shows the characteristic thickness of SOL plasma for the density λ_n and electron λ_T calculated from a simple competition of parallel and perpendicular transport for some values of density and temperature. The range of δ in the Case C configuration is shown in the figure as a dark bar. It is suggested from this figure that the divertor target plate should be designed to make the connection length less than 100 m. The value of λ is a function of $D_\perp$ or $\chi_\perp$, which are usually determined by anomaly diffusion. We assumed Bohm diffusion coefficient, $T/(16eB)$, for $D_\perp$ and $\chi_\perp$, in this calculation. The actual values of them, and their parameter dependence should be obtained through plasma experiments.

5. Discussions

In the helical divertor configuration (Case A), the divertor footprints are localized not only in the poloidal direction but also in the toroidal direction, in contrast to the helical divertor in Heliotron E, where the divertor trace continuously runs along the torus helically. Moreover, in Heliotron J, owing to rather short connection length, the edge field lines cross the wall before the ergodic feature of helical divertor configuration becomes apparent. On the other hand, in the Case B island divertor configuration, the edge field lines cross the wall before they make island structure perfectly and the footprints are also localized in poloidal and toroidal directions. Form the divertor operation viewpoint, there might be little difference between the both configurations except for the height of "X-point". It is necessary to artificially enhance the ergodicity by using external perturbation fields for the study of the "ergodic" field effects on SOL and divertor plasma transport.

All configurations discussed in this report will make divertor footprints localized in toroidal direction. Even in a conventional helical divertor case, however, particle and heat load is not uniform along the divertor trace [4]. Therefore, advantages and disadvantages for such a "local divertor" over a helically continuous divertor must be concluded after more detailed physical and technical investigations. It should be emphasized from a technical viewpoint that the accessibility to the divertor in the "local divertor" configuration presented here is better than the continuous helical divertor since the divertor footprints can locate in an outer open space.

Some of functions that a divertor should play are depends on "the machine size". For example, in Heliotron J, the short connection length from the "X-point" to the target plate such as in the Case A might be disadvantage for the remote cooling scenario of divertor operation. However, the connection length itself can be elongated by increasing the machine size or taking a proper design of the vacuum vessel. Therefore, a major objective of divertor study in a small device such as Heliotron J should be to make clear the relation between the edge field structure and basic properties of SOL/ divertor plasma.

6. Summary

Characteristics of edge magnetic field in Heliotron J are numerically investigated. Owing to the flexibility of field configuration control in Heliotron J, a helical (Case A) or island divertor (Case B, C) configuration

can be produced in the same device.

In the helical divertor configuration, the footprints of edge field lines on the wall are localized on some discrete regions in a torus. Owing to short connection length, the edge field lines cross the wall before their ergodic feature becomes apparent.

Two different modes, m/n = 8/4 (Case C) and 7/4 (Case B), of island divertor configurations are obtained depending on $\iota(a_p)/2\pi \sim 0.5$ and 0.57, respectively. In the Case B configuration, the center of island is far from the confinement region. A part of the island crosses the wall and the footprints of field lines are localized on two different regions per field period at low field side.

In these divertor configurations, parallel and anti-parallel flows of SOL plasma reach at different areas on the wall (or divertor plates). By adjusting a target position, we can guide the plasma flows to high or low field side.

In the m/n = 8/4 configuration, the center of island is close to the confinement region and the island does not cross the wall. By setting target plates at the island position, it is possible to design an island divertor such as a W7-X type or LID type.

Acknowledgement

The authors are grateful to the member of the Heliotron J Group for useful discussions and help. The authors are also grateful to Prof. N. Inoue, Director of Institute of Advanced Energy, for his continuing help and encouragement.

This work was partly supported by the Collaboration Program of the Laboratory for Complex Energy Process, Institute of Advanced Energy of Kyoto University.

References

[1] F. Sano *et al.*, J. Plasma Fusion Res. SERIES, Vol.**1**, 168 (1998).

[2] M. Wakatani *et al.*, in 17th IAEA Fusion Energy Conf. (Yokohama, Oct., 1998), IAEA-CN-69/ICP/08.

[3] T. Obiki *et al.*, in 12th Int. Stellarator Conf. (Madison, Oct., 1999). F. Sano, *et al.*, ibid.

[4] T. Mizuuchi *et al.*, J. Nucl. Mater., **162-164**, 105 (1989).